서울醫大學術誌 제25권 제 2 호
The Seoul Journal of Medicine
Vol. 25, No. 2, June 1984
ISSN 0582-6802

Estimation of Regional Cardiac Wall Stress From Biplane Coronary Cineangiograms

冠狀動脈 血管造影像을 利用한 局部心筋應力推定

Byoung G. Min, Hee C. Kim, Jong H. Park*, Myoung M. Lee*, Jung D. Seo*, Young W. Lee*, Man C. Han.**

Department of Biomedical Engineering, Internal Medicine, and Radiology,**
College of Medicine, Seoul National University.*

INTRODUCTION

The regional changes of cardiac wall deformation and the wall stress are important for evaluation of the myocardial functions. However, their application for clinical diagnosis has been limited, because it is difficult to measure these regional myocardial parameters in the intact heart.

Meier et al.(1980) and Walley et al. (1982) used the radiographic images of the implanted radiopaque markers in the beating heart to estimate the local twist and segmental shortening of small epicardial segment.

After elimination of the effects of the time-varying displacements of the overall cardiac motion using kinematic approaches, the local deformation was represented by the regional rotation tensor and the muscle wall stretch tensor. Also, the changes of wall thickness could be computed from the stretch tensor under the assumption of the isochoric deformation.

While the regional wall stress is known as one important contractile parameter of the muscle fiber in normal and abnormal cardiac functions, it has been difficult to measure the regional changes of wall stress. Sandler and Dodge (1963) studied the average stresses for an ellipsoidal model with finite wall thickness based upon Laplace's law (Laplace, 1805). Wong and Rautaharju (1968) estimated the stress distribution including the effects of shear and bending moments, which were shown to be negligible by Mirsky (1969).

In the present study, we evaluated whether the motion images of the coronary bifurcation points can be used for computation of the local deformation(金등, 1983) and the regional wall stress, thus avoiding thoracotomic procedures for implantation of markers. The local wall deformation and the regional wall stress were computed using the kinematic method of three feature points around the coronary bifurcation points.

This method utilizing the moving coronary bifurcation points as natural markers can increase the usefulness of the coronary cineangiography by providing the regional myocardial status in addition to the vessel's patency.

Usage of the coronary artery bifurcations for determination of the global epicardial displacements was previously investigated by Kong et al. (1971) and Potel et al. (1983). Kong's

+ 접수일자 : 1984. 2. 27.
* 本 研究는 1984년 서울大學校病院 臨床研究費 보조로 이루어진 것임.

results showed a close correlation between the spacial changes of bifurcations' interdistances and the implanted markers' displacements during a heart cycle. This result provided a basis of using the displacement data of the bifurcation points for computation of the cardiac wall thickness and the wall stress in the intact heart.

ANALYSIS

A. Representation of Regional Myocardial Motion

It has been shown (Meier et al., 1980) that the regional cardiac wall deformation can be approximated as homogeneous changes, and described by a linear tensor of gradient, T, in a small myocardial region. This deformation tensor, T, related the position data of feature points in the reference frame of the end-diastolic phase to those in the following sequential frames within a heart cycle. Also, this deformation tensor can be uniquely represented by the product of the orthonormal rotation tensor, R, and the positive symmetric stretch tensor, D, using a polar decomposition theorem (Meier et. al., 1980).

$$T=RD. \tag{1}$$

Therefore, when the instantaneous deformation tensor is calculated from the position data of the feature points, one can evaluate the numerical values of the tensors R and D uniquely. The tensor, R, provides a rotation angle, α. The eigenvalues of the stretch tensor, D, provides the epicardial strains and the tensor's eigenvectors show the principal shortening axes of the deformation.

B. Local Myocardial Coordinate System.

The global heart motion effects of translation, rotation, and torsion should be eliminated before analyzing the regional epicardial motion. In Meier et al.'s method, these overall motion effects were eliminated by the coordinate transformation method using the position data of the ventricular apex and the base. Since these position data are difficult to obtain for the same heart cycle in the coronary angiograms, we used the following approach based upon the simplified perspective coordinate transformation (Kim et. al., 1982).

In a small triangular plane composed of three feature points A,B,C located on the coronary artery tree, as shown in Fig. 1 (a), the time-varying centroid point, S, of the triangle ABC is computed in the external coordinate basis (x,y,z) during a heart cycle as follows;

$$S(t)=\{A(t)+B(t)+C(t)\}/3. \tag{2}$$

Since this centroid point moves together with the heart, the effects of global translation can be eliminated in a new coordinate system (x', y',z') with its origin located at the centroid point.

In the new coordinate system, three feature points A,B,C are represented as follow in Fig. 1(b),

$$\begin{aligned} A'(t)&=A(t)-S(t)\\ B'(t)&=B(t)-S(t)\\ C'(t)&=C(t)-S(t). \end{aligned} \tag{3}$$

Then, we can use the simplified perspective transformation method to transform the (x',y', z') coordinate system to the observer coordinate system (x'',y'',z'') where the z'' axis is parallel to the normal vector component, n', of the triangular plane ABC, as shown in Fig. 1(c). These transformation can be expressed as follows, using a homogeneous coordinate representation (Kim et al., 1982),

$$[x'', y'', z'', 1]=[x', y', z', 1]\cdot \begin{pmatrix} \frac{-b'}{R_2} & \frac{-a'c'}{R_1R_2} & \frac{-a'}{R_1} & 0\\ \frac{a'}{R_2} & \frac{-b'c'}{R_1R_2} & \frac{-b'}{R_1} & 0\\ 0 & \frac{R_2}{R_1} & \frac{-c'}{R_1} & 0\\ 0 & 0 & R_1 & 1 \end{pmatrix} \tag{4}$$

and $n'(t)=\{C'(t)-B'(t)\}\times\{A'(t)-B'(t)\}$,

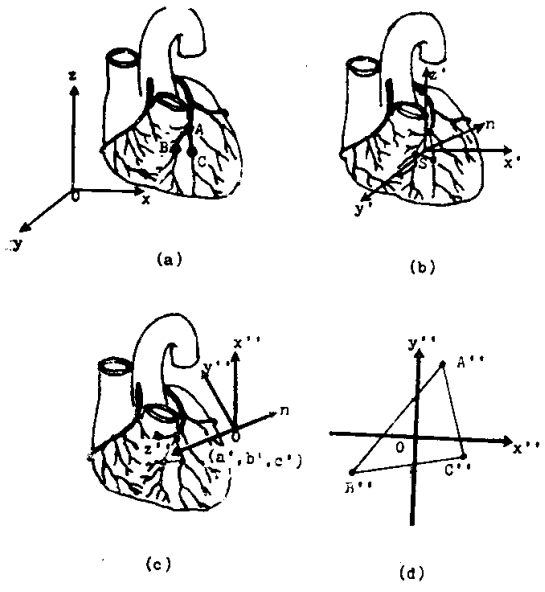

Fig. 1. Schematic diagram of the coordinate system transformation procedure for the elimination of the global heart motion;
(a) external camera coordinate system(x, y, z) and three feature points A, B, C,
(b) translated coordinate system(x', y', z') with its origin located at the centroid points S, and
(c) observer coordinate system(x'', y'', z'') with its origin on the normal vector component, n', of the ΔABC.

where (a', b', c') is an arbitrary viewing point on the normal vector $n'(t)$ in the (x', y', z') coordinate system,

$$R_1=(a'^2+b'^2+c'^2)^{\frac{1}{2}},$$

and $R_2=(a'^2+b'^2)^{\frac{1}{2}}$.

If the viewing position (a', b', c') has a fixed distance from the centroid, the z'' axis data will always have constant values of R_1 after the above perspective transformation. Then, the moving position data of the feature points can be represented by the two-dimensional values, as shown in Fig. 1(d).

C. Local Epicardial Deformation and Strains.

As the reference frame of the deformation tensor, T, is given at the end-diastolic phase, this tensor describes the time-varying ventricular deformation during a heart cycle relative to its end-diastolic shape and orientation. In this case, the matrix of the position data of three feature points, $W(t)$, can be expressed in the observer coordinate(x'', y'', z'') as follows;

$$W(t)=T(t)\cdot W_{ed}, \tag{5}$$

where

$$W(t)=[A''(t)\ \vdots\ B''(t)\ \vdots\ C''(t)]$$

$$=\begin{pmatrix} A_x''(t) & \vdots & B_x''(t) & \vdots & C_x''(t) \\ A_y''(t) & \vdots & B_y''(t) & \vdots & C_y''(t) \\ R_1 & \vdots & R_1 & \vdots & R_1 \end{pmatrix},$$

$$W_{ed}=[A_{ed}''\ B_{ed}''C_{ed}''],$$

and $A_e'_d', B_e'_d', C_e'_d'$ are the observer coordinate position data of three feature points at the end-diastolic phase. From Eq. (5), the deformation tensor, T, can be computed using the least squares estimation technique as follows(Walley et al., 1982),

$$\hat{T}(t)=W(t)\cdot W_{ed}{}^T\cdot(W_{ed}\cdot W_{ed}{}^T)^{-1} \tag{6}$$

Then, $\hat{T}(t)$ can be uniquely represented by the product of the R and D in Eq. (1), (Meier et al., 1980)

$$\hat{T}(t)=R(t)\cdot D(t) \tag{7}$$

$$\text{or}\begin{bmatrix} \hat{T}_{11}(t) & \hat{T}_{12}(t) \\ \hat{T}_{21}(t) & \hat{T}_{22}(t) \end{bmatrix}=\begin{bmatrix} \cos\alpha(t) & -\sin\alpha(t) \\ \sin\alpha(t) & \cos\alpha(t) \end{bmatrix}\cdot \begin{bmatrix} D_{11}(t) & D_{12}(t) \\ D_{12}(t) & D_{22}(t) \end{bmatrix},$$

where $\alpha(t)$ is the local twist angle.

By solving the above simultaneous equations, one can obtain the numerical values of the rotation tensor, $R(t)$, and the stretch tensor, $D(t)$, from the estimated tensor $\hat{T}(t)$. Then, the epicardial strains in the principal direction can be computed from the eigenvalues$(\lambda_1(t),\ \lambda_2(t))$ and the eigenvectors$(\rho_1(t),\ \rho_2(t))$ of the tensor $D(t)$ (Meier et al., 1980).

D. Local Wall Thickness and Regional Wall Stress

Under the assumption of the isochoric or volume preserving deformation, the third eigenvalue of the three-dimensional stretch tensor $(\lambda_3(t))$ must satisfy the following relationship

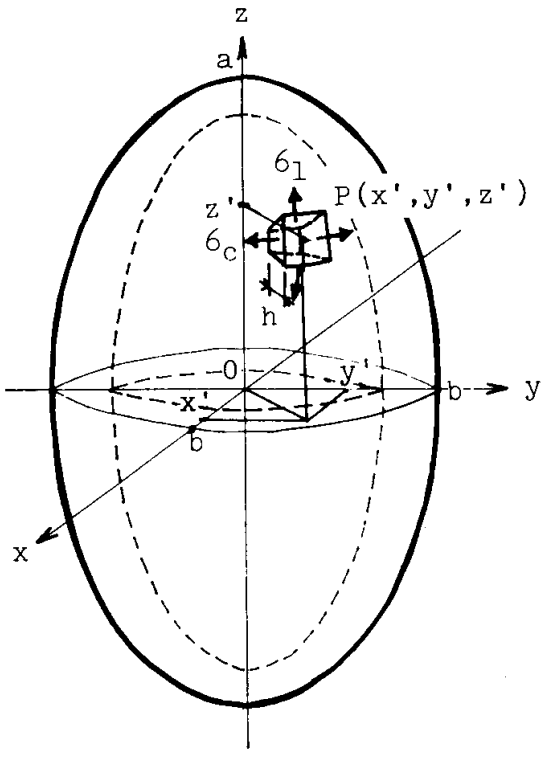

Fig. 2. Ellipsoidal model of the thick-walled left ventricle for the computation of the regional longitudinal(σ_l) and circumferential(σ_c) wall stress of the cardiac wall segment at $P(x', y', z')$.

(Meier et al., 1980),

$$\lambda_1(t)\cdot\lambda_2(t)\cdot\lambda_3(t)=1. \quad (8)$$

The radial strain of regional myocardium ($\lambda_3(t)-1$) can be estimated from the epicardial strains ($\lambda_1(t)-1$, $\lambda_2(t)-1$). Then, the instantaneous regional wall thickness can be computed as,

$$h(t)=h_{ed}\lambda_3(t), \quad (9)$$

where h_{ed} is the wall thickness at end-diastole.

We used a thick-walled left ventricular ellipsoidal model (Falsetti et al., 1970) as shown in Fig. 2 for computation of the longitudinal regional wall stress (σ_l) and the circumferential wall stress (σ_c) in the following equations. The derivation of these equations is summarized in the Appendix.

$$\sigma_l=\frac{Py'r}{h(h+2y')}. \quad (10)$$

$$\sigma_c=\frac{P}{h}\left[1-\frac{(2r+h)y'r}{2Rr(h+2y')}\right]\frac{2Rr}{2R+h}$$

where a=base-to-apex semiaxis, b=minor semiaxis, P=left ventricular pressure, h=regional wall thickness as computed in Eq. (9),

$$r=\frac{(a^4y'^2+b^4z'^2)^{\frac{1}{2}}}{a^2},$$

$$R=r^3\frac{a^2}{b^4},$$

$$y'=\sqrt{(1-f_z^2)}\cdot b, \text{ and } z'=f_z\cdot a(-1<f_z<1).$$

METHOD

A. Coronary Cineangiography

The present algorithms for the regional myocardial motion were tested using the biplane coronary cineangiograms obtained during the diagnostic evaluation of a patient's coronary circulation. The M-mode echocardiogram was recorded with 2.25MHz focused transducers, and HITACHI EUB 10A echographs on stripchart recorders several days before catheterization. The left ventriculogram and the left ventricular pressure waveforms were obtained using the two catheters located in the left ventricle, one for injection of contrast medium and the other for pressure measurement by Statham P23Db transducer. They were inserted through the femoral artery by the Seldinger technique. A bolus of radiopaque contrast media (Telebrix 60®) was injected using a power injector(Medrad, Mark IV) at an injection rate of 15ml/sec for a total amount of 45ml. The electrocardiogram and left ventricular pressure were recorded using HP's 8-channel recording system(8890B). The third catheter was located selectively in the coronary sinus for coronary angiography with a hand injection technique for a total amount of 7ml. After each injection of contrast media, a plastic plate of 15cm×15cm containing 10×10 pieces of 0.05-inch lead shot embedded with 1cm interval was imaged for calibration

of the biplane views of the angiograms.

The angiographic system used in the present study consists of an X-ray generator (G.E., MSI-1250/v, 1000MA), image intensifier(9 in. circular, cesium iodide), plumbicon camera, and cinematograph(ARRITECHNO 35) with 35-mm film at the rate of 60 frames per second.

B. Data Collection

Using a Vanguard 35-mm motion analyzer (XR-3), a digitizing pad(HIPAD™), and DEC PDP-11/03 MINC microcomputer, each view of cineangiogram was digitized, and calibrated. The three-dimensional coordinate data were reconstructed to the fixed external camera coordinate system based upon the orthogonal projection. The three feature points were selected on the left anterior descending(LAD) branch of the coronary artery vessels, two bifurcation points and one inflection point between them as shown in Fig. 3(C). All data were collected within the first four beats after injection of contrast media.

Also, the recorded left ventricular pressure waveform and the echocardiogram were digitized

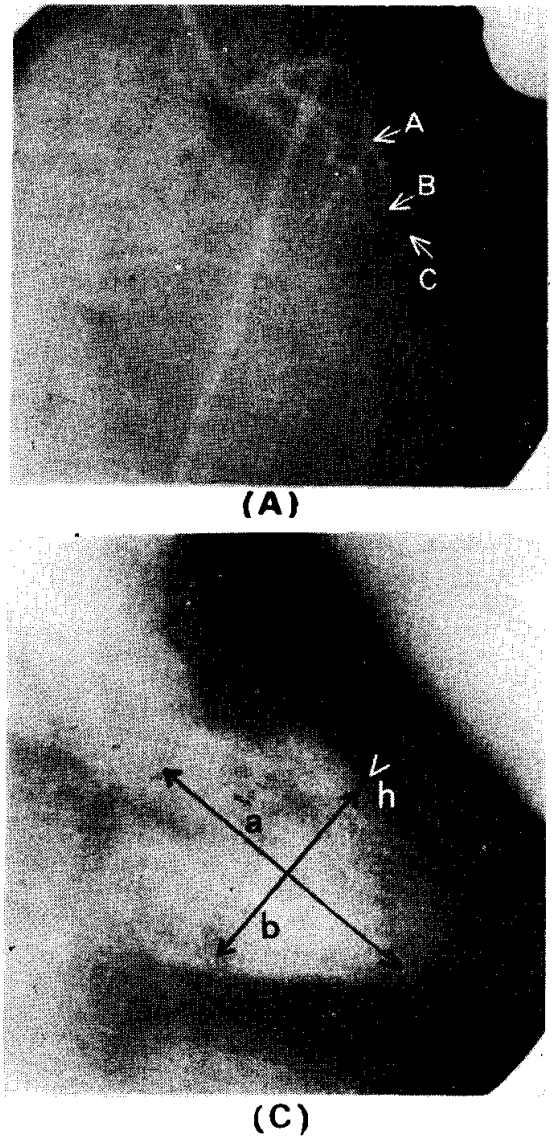

Fig. 3. A normal patient's cineangiograms used for application of the present algorithm;
(A) RAO 30° view of the left anterior descending coronary with the three feature points *A*, *B*, *C*,
(B) LAO 60° view of the same vessel, and
(C) RAO 30° view of the left ventricular chamber with major axis, minor axis, and wall thickness.

and used as input data for computation of the regional wall thickness and stress.

RESULTS

Fig. 3(A) and 3(B) show a normal subject's biplane coronary cineangiograms in RAO 30° and LAO 60° directions, respectively. Using these biplane angiograms, the perspective trans formation technique of Eqs. (3) and (4) was applied to the three feature points A, B, C corresponding to the two bifurcation points and an inflection point on the LAD branch as shown in Fig. 3(A) and 3(B). The same patient's left ventriculogram is shown in Fig. 3(C) for RAO 30° direction together with its major, minor axes and wall thickness at the end-diastolic phase. The time variation of the major axis, minor axis and the left ventricular pressure are shown in Fig. 4(a), 4(b), and 4(c), respectively during two consecutive heart cycle. The end-diastolic pressure was 12mmHg, and the peak systolic pressure was 140mmHg.

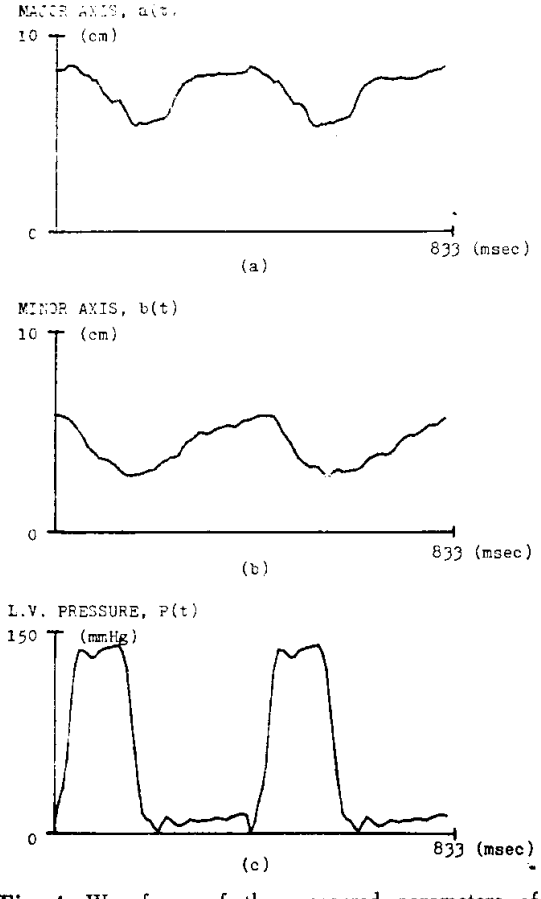

Fig. 4. Waveforms of the measured parameters of (a) major axis, (b) minor axis, and (c) left ventricular pressure.

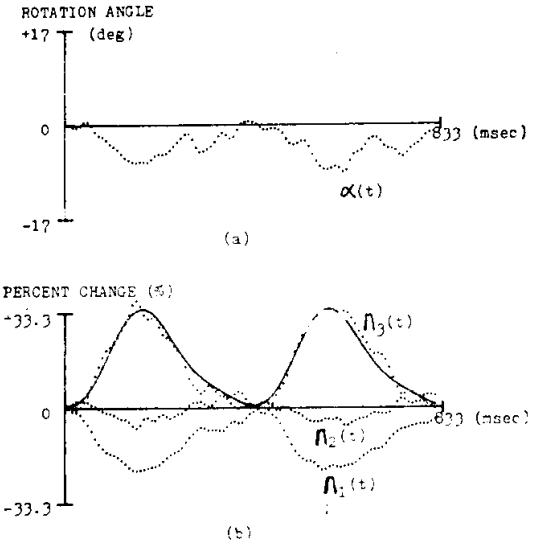

Fig. 5. Computed waveforms of the present regional epicardial deformation analysis;
(a) local twist angle, $\alpha(t)$,
(b) percentage changes of the epicardial strains ($\Lambda_1(t)$, $\Lambda_2(t)$) and the radial strain ($\Lambda_3(t)$) with its fitted curve.

After the present regional epicardial deformation analysis, the local twist angle, $\alpha(t)$, was computed as shown in Fig. 5(a). As the positive values of α shows the counterclockwise rotation in Eq. (7), the computed negative angles indicate that the local twist occurred within a clockwise rotation. The local segment was shown to be rotated with its maximum value at the peak systolic pressure, and returned slowly to the original position.

The percentage changes of the epicardial strain was computed and is shown in Fig. 5(b) using the stretch tensor's eigenvalues as follows;

$$\Lambda_1(t) = (\lambda_1(t) - 1) \times 100(\%) \quad (11)$$
$$\Lambda_2(t) = (\lambda_2(t) - 1) \times 100(\%)$$

The major shortening($\Lambda_1(t)$) has a large change(22%) at the peak systolic pressure phase, and its waveform is shown to be similar to the measured changes of minor axis of Fig. 4(b). The local wall thickening was computed as the strain in the radial direction($\Lambda_3(t)$), as it was computed from the third eigenvalue of $\lambda_3(t)$ in Eq. (8) as follows;

$$\Lambda_3(t)=(\lambda_3(t)-1)\times 100(\%) \qquad (12)$$

As shown in Fig. 5(b), the maximum percentage changes of the local wall thickness was 37.8%.

Using the least square error curve fitting method, a smoothed curve of the wall thickening was obtained.

After calibrating with the measured wall thickness at end-diastole phase using the M-mode echocardiogram and left ventriculogram, the absolute values of the local wall thickness were obtained.

The regional wall stress around the midwall section was computed using Eq. (10) with f_z= 0.3 for its location. As compared with the measured left ventricular pressure in Fig. 6, the

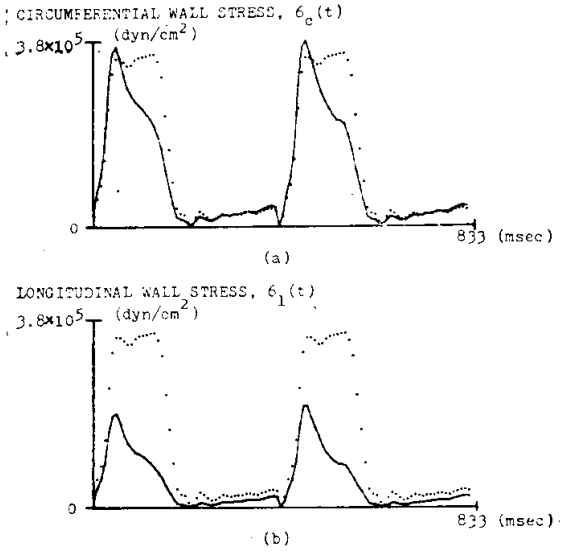

Fig. 6. Waveforms of the regional (a) circumferential and (b) longitudinal wall stress around the midwall section with f_z=0.3 for its location.

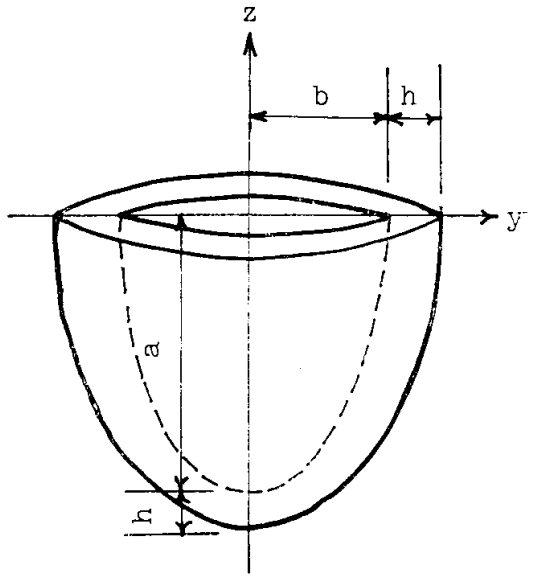

Fig. 7. Truncated ellipsoidal model of left ventricle used to simulate the regional stress at various points.

computed wall stress shows early diminution after its peak value while the left ventricular pressure continues to rise during the systolic phase. This observation is similar to the other reported results (Sandler et. al., 1963; Wong et. al. 1968; Falsetti et. al., 1970). The peak circumferential and longitudinal stresses were 3.79×10^5(dyn/cm²), 2.06×10^5(dyn/cm²), respectively.

Using Eq. (10), the regional stress at various points of the truncated ellipsoidal left ventricle was computed as shown in Fig. 7. In this computation, the measured left ventricular pressure, the major and minoraxes were used. Also, the wall thickness(h) was calculated by following equations, when the changes of the wall thickness are same along the whole ventricle with the isochoric deformation at every instant during one heart cycle,

$$\frac{4}{3}\pi[\{a(t)+h(t)\}^2\cdot\{b(t)+h(t)\}]-\frac{4}{3}\pi[a(t)^2\cdot b(t)]=\text{const.} \qquad (13)$$

When the diastolic phase is seleced as a ref-

erence frame at $t=0$, the wall thickness $h(t)$ must satisfy the following third order equation with respect to the time-varying constant parameters of $a(t)$ and $b(t)$ of the major and minor semi-axes,

$$[h(t)^3+\{2a(t)+b(t)\}h(t)^2+\{a(t)+2b(t)\}a(t)h(t)]-[h(0)^3+\{2a(0)+b(0)\}h(0)^2+\{a(0)+2b(0)\}a(0)h(0)]=0 \quad (14)$$

A real solution of Eq. (14) is given as the wall thickness and shown in Fig. 8. The computed distribution of the circumferential and longitudinal stress from the base to apex are shown in Fig. 9, and the results are similar to the previously reported distributions(Wong et al., 1968).

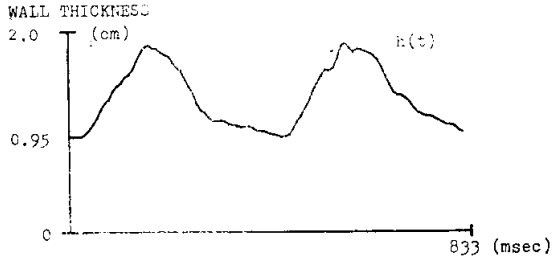

Fig. 8. Waveforms of the wall thickness obtained under the assumption of the isochoric contraction during two heart cycles and used for the regional stress simulation

DISCUSSION

A new mathematical method was developed to estimate local epicardial deformation, wall thickness, and the regional wall stress using biplane coronary cineangiograms of a normal patient. The present algorithm is a further development of the previous results that the bifurcations of coronary arteries could provide natural landmarks of the epicardial dimensional changes, and one other result that the motion image of the markers could provide the regional wall defomation(Meier et. al., 1980; Kong et. al., 1971). It was previously shown that the epicardial segment dimensional changes were not affected by intracoronary injection of contrast medium less than 25ml in the first 5 to 6 cardiac cycles(Kong et. al., 1971; Potel et. al., 1983). Thus, the objective of the present study was to increase clinical utilization of coronary angiography by providing myocardial informations including regional stress distribut-

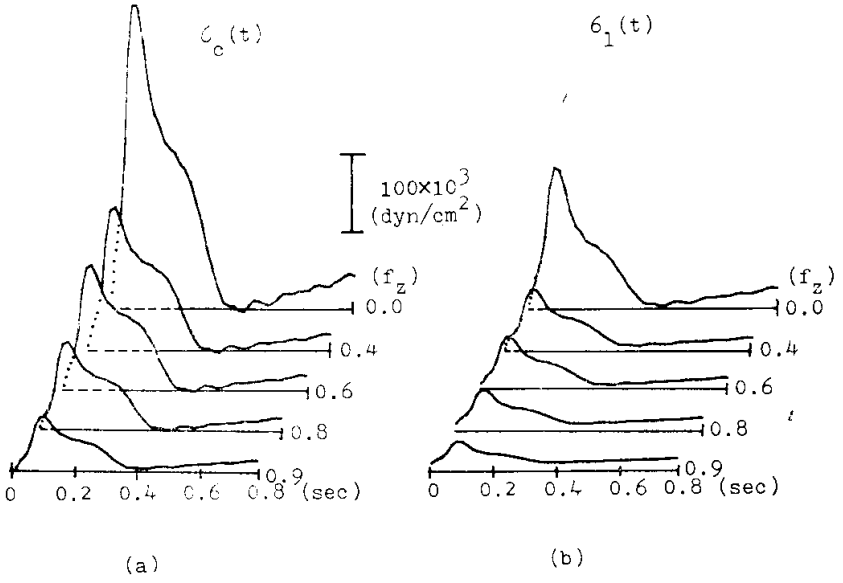

Fig. 9. Waveforms of the computed distribution of the (a) circumferential and (b) longitudinal wall stress from the base($f_z=0.0$) to apex ($f_z=1.0$) of the truncated ellipsoidal left ventricle.

ion. Previously, the difficulties in measuring the regional changes of wall thickness using conventional left ventriculograms or echocardiograms have prevented calculation of the regional wall stress(Hood et.al., 1969). In the present study, the biplane image analysis method was developed to estimate the regional stress with less complexities than the previous methods, but the estimation results show its validity of the present method, as compared with the previous results (Wong et. al., 1968).

Because our model is based upon the geometric assumption of left ventricle as an ellipsoid of revolution, the calculated stresses provides its values under the condition that the same stress was developed at any point on the cross-sectional plane perpendicular to the major axis. Therefore, only one parameter, f_z, in Eq. (10), which is a position factor of a specific cross-section on the major axis, is necessary to locate the region of interest on the ellipsoid.

The present algorithm has several advantages for the clinical applications: First, the regional changes of deformation and wall stress of myocardium can be achieved after eleimination of the global effects. These have been difficult to obtain in the conventional methods. Second, the data collection is relatively easy, and the procedure is safer than any other method including the marker implantation method, which was thought to be the most reliable technique for estimation of epicardial motion. Third, the clinical evaluation of these regional myocardial changes together with the deficiency of the blood supply in one diagnostic procedure may be very useful for early detection of the impaired region around the coronary arteries. Also, it may be useful to evaluate the clinical significance of the region with normal wall stress while the region is supplied with the narrowed blood vessels.

Our algorithm has the following possible limitations: First, any sliding effects between the bifurcation points and the myocardium may exist depending upon the degree of coupling, and it must be considered. While a close correlation was reported (Kong et. al., 1971) between the position data of the bifurcations and the metal markers points, other feature points, such as inflection points, may affect the results. With improved image quality of the biplane coronary cineangiogram, these problems can be avoided by using only the bifurcation points for analysis. Second, when the blood supply is severely obstructed due to arterial occlusion, the tracing of the feature points will be difficult.

In conclusion, the present method provides a new technique of evaluating the regional wall deformation and wall stress together with the blood vessel conditions in a single coronary cineangiography procedure.

APPENDIX

Calculation of the Regional Stress of a Thick Ellipsoid of Revolution.

Laplace's law for a thick-walled shell as shown in Fig. 10 may be written in terms of two stress components, σ_c and σ_l (Falsetti et. al., 1970).

$$\frac{P}{h}=\frac{2R+h}{2Rr}\sigma_c+\frac{2r+h}{2Rr}\sigma_l. \qquad \text{(A1)}$$

where r and R are the principal radii of curvature, σ_c and σ_l are the circumferential and longitudinal stress components, respectively, P is left ventricular pressure, and h is the regional wall thickness. If the

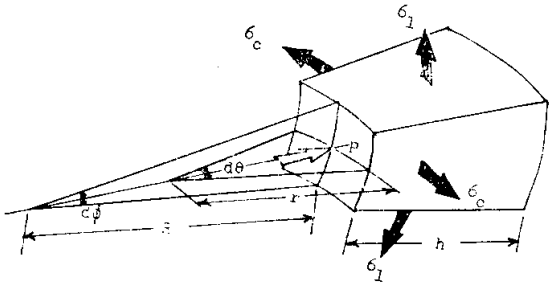

Fig. 10. A thick-walled left ventricular wall segment with the principal radii of curvature R and r.

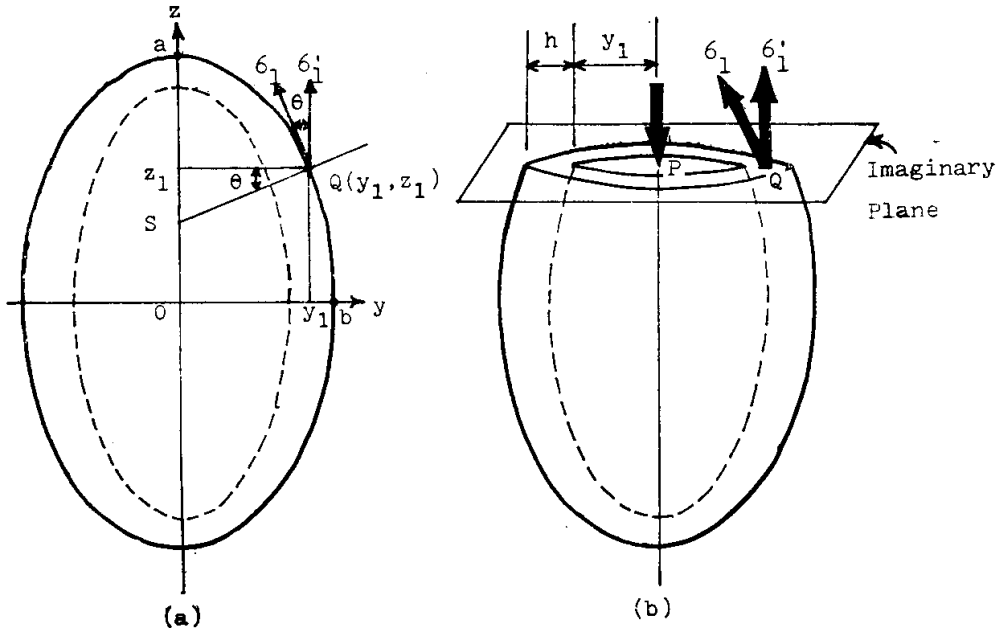

Fig. 11. Thick-walled ellipsoidal model of left ventricle;
(a) relationship between the stress components in the two-dimensional plane, and
(b) total force balance condition between the pressure in the cavity and the wall stress on the cross-imaginary plane.

wall is thin, Eq. (A1) reduces to the Sandler and Dodge's equation (Sandler et. al., 1963).

$$\frac{P}{h}=\frac{\sigma_c}{r}+\frac{\sigma_l}{R} \tag{A2}$$

In Eq. (A1), to determine absolute values of each stress at a specific point, three parameters(r, R, and σ_c (or σ_l)) must be known in addition to P and h. The principal radii of curvature at any point on an ellipsoid of revolution with the general form such as,

$$b^2x^2+b^2y^2+a^2z^2=a^2b^2, \tag{A3}$$

where a and b are major and minor semi-axial lengthes, respectively, and the major axis is on the z axis, can be represented as(Timoshenko, 1959);

$$R=r^3\frac{a^2}{b^4},\quad r=\frac{(a^4y^2+b^4z^2)^{1/2}}{a^2} \tag{A4}$$

For a point at the equator of the ellipsoid, Eq. (A4) can be redued to,

$$R=\frac{a^2}{b},\quad r=b. \tag{A5}$$

From now on, we will consider the elliptical points on $x=0$ plane, i.e. $y-z$ plane, for simplicity of analysis without losing the generality because of symmetricity of the ellipsoid of revolution. In this case, the ellipse on $y-z$ plane is represented as shown in Fig. 11(a),

$$\frac{y^2}{b^2}+\frac{z^2}{a^2}=1, \tag{A6}$$

and the coordinates of an arbitrary point $Q(y_1, z_1)$ can be located with a fraction f_z,

$$z_1=f_z\cdot a\ (-1<f_z<1) \tag{A7}$$
$$y_1=f_y\cdot b=\sqrt{(1-f_z^2)}\cdot b.$$

Then, using simple geometric calculations of two-dimensional ellipse, one can determine the longitudinal stress σ_l at apoint Q. From Fig. 11(b), the total force balance condition between the pressure in the cavity and wall stress on the cross-sectional imaginary plane which includes the point Q and perpendicular to the major axis, must be satisfied as (Hefner et. al., 1962),

$$P\cdot\pi\cdot y_1^2=\sigma_l'\cdot\pi\{(y_1+h)^2-y_1^2\},$$
$$\text{or}\quad \sigma_l'=\frac{Py_1^2}{h(2y_1+h)}, \tag{A8}$$

where y_1 is given in Eq. (A7) and σ_l' is the vertical component of σ_l and other parameters are as defined above. Using the equation of normal line SQ at point Q in Fig. 11(a), the geometric relation between σ_l and σ_l' can be represented as,

$$\sigma_l=\sigma_l'/\cos\theta,$$

where $\cos\theta=\frac{a^2y_1}{(a^4y_1^2+b^4z_1^2)^{1/2}}=\frac{y_1}{r}$. (A9)

From Eqs. (A8) and (A9), the longitudinal stress at a point Q is given by,

$$\sigma_l=\frac{Py_1r}{h(h+2y_1)} \quad \text{(A10)}$$

Then, the circumferential stress σ_c at a point$Q(y_1, z_1)$ can be determined from the Eq. (A1) and Eq. (A10),

$$\sigma_c=\frac{P}{h}\left\{1-\frac{(2r+h)y_1r}{2Rr(h+2y_1)}\right\}\frac{2Rr}{2R+h}, \quad \text{(A11)}$$

where all parameters are defined previously.

SUMMARY

A new mathematical method was developed to estimate the local epicardial deformation, wall thickness, and the regional circumferential and longitudinal wall stress using biplane coronary cineangiograms. In this method, the motion images of the coronary artery bifurcation points were used as natural landmarks for the kinematic analysis of the ventricular deformation. In a normal patient's coronary cineangiograms, the estimation results show the validity of th present analysis, compared with the previous results based upon the implanted markers. Therefore, it provides a new method of evaluating the regional wall deformation and wall stress together with the blood vessel conditions using the coronary cineangiaphy procedure.

＝國文抄錄＝

冠狀動脈血管造影像을 利用한 局部心筋應力推定

서울大學校 醫科大學 醫工學科,
內科學敎室* 및 放射線科學敎室**
閔丙九 · 金喜贊 · 朴鍾勳* · 李命默*
徐正燉 · 李迎雨* · 韓萬靑**

본 연구에서는 저자들에 의해 이미 발표된 바와 같이 (金, 1983) 관상동맥 혈관조영상에서 관상동맥 분지점의 시간에 따른 위치변화로부터 국부심근의 변형을 심근의 두께 변화와 함께 해석하였고, 동시에 좌심실 벽의 국부심근에 작용하는 응력(Stress)의 추정을 시도하여 정상적인 관상동맥을 갖고 있는 환자의 혈관조영상을 처리한 결과와 반타원체 모델의 좌심실에 대한 시뮬레이션(Simulation) 결과를 제시하였다. 환자 데이타의 처리에서는 국부심근의 수축 및 이완에 따르는 변형을 회전과 수축, 그리고 두께 변화의 요소들로 분해하고, 이에 작용하는 원주방향(Circumferential) 및 길이방향(Longitudinal)의 응력을 계산하여 정량적인 수치들로 제시하였고, 시뮬레이션을 실시하여 좌심실 벽에 작용하는 두 성분의 응력에 대한 각 위치에 따른 분포를 얻어 이미 보고된 다른 연구 결과와 잘 일치함을 확인하였다. 좌심실 심근의 수축상태를 나타내는 중요한 변수로서 응력을 비교적 간단한 방법으로 국부적인 값까지 얻을 수 있다는 것외에 이러한 해석의 기본 데이타를 관상동맥의 분지점으로부터 얻었으므로 관상동맥의 異常과 심근운동과의 관계를 고려할 때 중요한 진단방법으로 기대된다.

REFERENCES

金喜贊, 閔丙九, 朴在亨, 韓萬靑：冠狀動脈血管造影像을 이용한 心筋운동해석에 관한 硏究. 서울의대학술지, 24(1)：143, 1983.

Falsetti, H.L., Mates, R.E., Grant, C., Greene, D.G. and Bunnell, I.L.: *Left ventricular wall stress calculated from one-plane cineangiography. —An approach to forcevelocity analysis in man. Circ. Res.*, 26：*71, 1970.*

Hefner, L.L., Sheffield, L.T., Cobbs, G.C. and Klip, W.: *Relation between mural force and pressure in the left ventricle of the dog. Circ. Res.*, **11**：*654, 1962.*

Hood, W.P., Jr., Thomson, W.J., Rackley, C.E. and Rolett, E.L.: *Comparison of calculations of left ventricular wall stress in man from thin-walled and thick-walled ellipsoidal models. Circ. Res.*, **24**：*575, 1969.*

Kim, H.C., Min, B.G., Lee, T.S., Lee, C.W., Park, J.H. and Han, M.C.: *Three-dimensional digital subtraction angiography. IEEE Trans. Med. Imag.*, **MI-1**(*2*)：*152, 1982.*

Kong, Y., Morris, J.J. and McIntosh, H.D.: *Assessment of regional myocardial performance from biplan e coronary cineangiograms. Am. J. of Cardiol.*,

27 : *529, 1971.*

Laplace, P.S.: *Theorie de laction capillaire. In Traite de Mecanique Celeste, Supplement au livre* **10**, *Paris, Couroien, 1805.*

McHale, P.A. and Greenfield, J.C.: *Evaluation of several geometric models for estimation of left ventricular circumferential wall stress. Circ. Res.*, **33** : *303, 1973.*

Meier, G.D., Ziskin, M.C., Santamore, W.P. and Bove, A.A.: *Kinematics of the beating heart, IEEE Trans. Biomed. Eng.*, **BME-27**(*6*) : *319, 1980.*

Mirsky, I.: *Left ventricular stresses in the intact human heart. Biophys. J.*, **9** : *189, 1969.*

Potel, M.J., Rubin, J.M., MacKay, S.A., Aisen, A. M., Al-Sadir, J. and Sayre, R.E.: *Methods for evaluating cardiac wall motion in three dimensions using bifurcation points of the coronary arterial tree. Invest. Radiol.*, **18** : *47, 1983.*

Sandler, H. and Dodge, H.T.: *Left ventricular tension and stress in man. Circ. Res.*, **13** : *91, 1963.*

Timoshenko, S.: *Theory of plates and shells. ed. 2, New York, McGraw-Hill Book Company Inc.*, : *440, 1959.*

Walley, K.R., Grover, M., Raff, G.L., Benge, J.W., Hannaford,B. and Glantz, S.A.: *Left ventricular dynamic geometry in the intact and open chest dog. Circ. Res.*, **50** : *573, 1982.*

Wong, A.Y.K. and Rautaharju, P.M.: *Stress distribution within the left ventricular wall approximated as a thick ellipsoidal shell. Am. Heart J.*, **75** : *649, 1968.*